SUPPLEMENTARY MATERIALS GUIDE

Tables

Supplementary Table 1. Clinical characteristics
Supplementary Table 2. *KRAS* assessment
Supplementary Table 3. Tumor burden and CEA data
Supplementary Table 4. Probabilities that mutations were absent in metastases prior to panitumumab therapy
Supplementary Table 5. Wild-type and mutant-specific primers
Supplementary Table 6. Total circulating cell-free DNA levels

Figures

Supplementary Fig. 1. Ligation and BEAMing assays used to detect circulating *KRAS* mutations. **a, b, c**, Each lane represents the results of ligation of one of six independent *KRAS*-specific PCR products, each containing 100 template molecules from the indicated patients' pre-treatment serum samples. The wild-type ligation products contain 6-carboxyfluorescein-labeled oligonucleotide probes that ligate to an unlabeled oligonucleotide only when wild-type alleles are present. The mutant (MUT) ligation products contain hexachlorofluorescein-labeled oligonucleotide probes that ligate to the same unlabeled oligonucleotide only when mutant alleles are present. The fluorescent images of denaturing acrylamide gels in which the ligation products were size-separated are shown. **d, e, f,** *KRAS*-specific PCR products were used as templates for BEAMing in which each template was converted to a bead containing thousands of identical copies of the template[12]. After hybridization to Cy3- or Cy5-labeled oligonucleotide probes specific for wild-type or mutant sequences, respectively, the beads were analyzed by flow cytometry. Beads whose fluorescence spectra lie between the wild-type and mutant-containing beads result from inclusion of both wild-type and mutant templates in the aqueous nanocompartments of the emulsion PCR. See Materials and Methods for additional details. **a, d**: Patient #17; **b, e**: Patient #20; **c, f**: Patient #28. The mutant probes used in **a, b, d,** and **e** were specific for *KRAS* cDNA nt 38A and the mutant probe used in **c** and **f** was specific for *KRAS* cDNA nt 35A. The fraction of beads representing mutant templates are indicated for each patient.

Supplementary Fig. 2. Time course of ctDNA, CEA, and tumor burden for all the patients in which ctDNA was detected (other than Patients 1 and 12, which are depicted in Fig. 1). Tumor burden refers to the aggregate cross-sectional diameter of the index lesions.

Supplementary Fig. 3. Kaplan-Meier Estimates of progression free survival in three groups of patients treated with panitumumab. (*Black*) patients whose tumors were *KRAS* mutant prior to initiating therapy, (*Red*) patients whose tumors were wild-type for *KRAS* prior to starting therapy with panitumumab and *did not* develop detectable secondary mutation in *KRAS*, and (*Blue*) patients whose tumors patients whose tumors were wild-type for *KRAS* prior to starting therapy with panitumumab and *did* develop a detectable mutation in *KRAS*. The progression-free survival was not different among patients who did or did not develop *KRAS* mutations during treatment (Hazard ratio 0.9; 95% CI 0.3366 to 2.453; p=0.85; Log-Rank Test).

Other

Supplementary Appendix. Mathematical modeling

Supplementary Table 1. Clinical characteristics

	Clinical and Demographic Info						Prior Therapy					Metastatic lesions prior to Panitumumab therapy	Response to Panitumumab		
Patient #	Age	Gender	ECOG PS[1]	Primary Site	Race/Ethnicity	Weeks since diagnosis of metastatic CRC	Lines of Prior Therapy	Chemotherapeutic agents	Biologic Therapy	Surgery (Intent)	Radiation Therapy	Number of lesions detectable by CT	WHO[2] RESPONSE	Progression Free Survival (weeks)	Overall Survival (weeks)
1	64	M	1	Colon	White/Caucasian	93	3	Cape, OXAL, IRT		Resection (Curative)		12	SD	33	33
2	53	M	0	Colon	White/Caucasian	96	3	5FU, LV, Cape, OXAL, IRT		Resection (Staging)		6	PR	22	76
*3**	*60*	*M*	*1*	*Colon*	*White/Caucasian*	*97*	*2*	*5FU, LU, IRT*		*Resection (Curative)*		*3*	*PD*	*7*	*119*
4	67	F	0	Colon	African American	105	3	5FU, LV, OXAL, IRT		Bypass (Palliative)	Pelvis (49 Gy)	2	SD	11	51
5	78	F	0	Colon	White/Caucasian	156	2	5FU, LV, OXAL, IRT	Bevacizumab	Resection (Curative)		4	PR	23	97
6	63	F	1	Colon	White/Caucasian	92	3	5FU, LV, OXAL, IRT	Bevacizumab	Bypass (Palliative)	Pelvis (58 Gy)	4	SD	35	35
7	55	M	1	Rectum	White/Caucasian	194	2	5FU, LV, Cape, OXAL, IRT	Bevacizumab	Resection (Curative)		7	SD	23	77
*8**	*48*	*F*	*1*	*Colon*	*White/Caucasian*	*68*	*2*	*5FU, LV, OXAL, IRT*	*Bevacizumab*	*Resection (Palliation)*		*3*	*PD*	*11*	*50*
9	50	M	1	Rectum	White/Caucasian	115	2	5FU, LV, Cape, OXAL, IRT		Resection (Palliation)	Pelvis (54 Gy)	9	PD	31	86
10	67	M	1	Colon	White/Caucasian	71	2	5FU, LV, OXAL, IRT		Resection (Palliation)		3	SD	23	113
11	52	M	1	Rectum	African American	48	2	5FU, LV, OXAL, IRT			Rectum (65 Gy)	9	PD	7	58
12	49	M	0	Colon	White/Caucasian	129	3	5FU, LV, Cape, OXAL, IRT	Bevacizumab	Resection (Palliation)		4	SD	23	75
13	59	F	1	Colon	White/Caucasian	61	2	5FU, LV, OXAL, IRT	Bevacizumab	Resection (Palliation)		7	SD	23	57
14	73	M	0	Colon	White/Caucasian	97	3	5FU, LV, OXAL, IRT		Resection (Curative)		4	PR	23	133
15	58	M	0	Rectum	White/Caucasian	151	3	5FU, LV, OXAL, IRT			Pelvis (51 Gy)	14	PR	25	25
16	72	F	1	Colon	White/Caucasian	86	3	5FU, LV, Cape, OXAL, IRT		Resection (Curative)		5	PR	23	45
17	57	F	1	Colon	White/Caucasian	67	2	5FU, LV, OXAL, IRT	Bevacizumab	Resection (Curative)	Pelvis (34Gy)	7	PR	31	83
18	47	F	0	Rectum	White/Caucasian	84	2	5FU, LV, OXAL, IRT	Bevacizumab			6	PR	28	88
19	42	M	0	Rectum	White/Caucasian	99	2	5FU, LV, Cape, OXAL, IRT	Bevacizumab	Resection (Curative)	Pelvis/Rectum (49 Gy)	2	PR	15	120
*20**	*56*	*F*	*1*	*Colon*	*African American*	*62*	*2*	*5FU, LV, OXAL, IRT*	*Bevacizumab*	*Resection (Curative)*		*5*	*PD*	*7*	*55*
21	57	M	0	Colon	White/Caucasian	106	2	5FU, LV, Cape, OXAL, IRT	Bevacizumab	Resection (Palliation)		10	SD	15	74
22	59	F	1	Colon	White/Caucasian	102	3	5FU, LV, Cape, OXAL, IRT	Bevacizumab	Resection (Palliation)		13	SD	15	25
23	69	M	1	Rectum	White/Caucasian	199	3	5FU, LV, Cape, OXAL, IRT		Resection (Curative)	Pelvis (50Gy)	9	SD	49	49
24	57	M	0	Unknown	African American	52	2	5FU, LV, OXAL, IRT	Bevacizumab	Resection (Curative)	Pelvis (50Gy)	12	SD	52	52
25	47	F	0	Colon	White/Caucasian	96	2	5FU, LV, OXAL, IRT	Bevacizumab	Resection (Palliation)		9	SD	20	67
26	59	F	0	Colon	White/Caucasian	132	3	5FU, LV, OXAL, IRT	Bevacizumab	Resection (Staging)		3	SD	23	130
27	73	M	0	Rectum	White/Caucasian	134	3	5FU, LV, Cape, OXAL, IRT	Bevacizumab	Excision (Curative)	Pelvis (54Gy)	6	SD	23	102
*28**	*78*	*F*	*1*	*Colon*	*White/Caucasian*	*232*	*3*	*5FU, LV, OXAL, IRT*	*Bevacizumab*	*Resection (Curative)*		*8*	*PD*	*7*	*36*

*Denotes patients (#3, 8, 20 and 28) whose tumor tissue was found to be KRAS mutant

[1]ECOG PS - Eastern Cooperative Group Perfomance Status (0 - Fully active without restriction; 1 - Restricted in physically strenuous activity and able to carry out work of a light or sedentary nature; 2 - Ambulatory and capable of all selfcare but unable to carry out any work activities; 3 - Confined to bed or chair more than 50% of waking hours; 4 - Totally confined to bed or chair; 5 - Dead)

[2]WHO Tumor Response Criteria (SD - Stable Disease; PD - Progressive Disease; PR - Partial Response; CR - Complete Response)

Supplementary Table 2. *KRAS* assessments

	Baseline *KRAS* Status	**Circulating Mutant *KRAS* Status***		**Circulating Mutant *KRAS* (fragments/mL)***								
Patient #	Tumor Genotype	Mutant *KRAS* Alleles Detected at Baseline	Secondary Circulating Mutant *KRAS* Alleles Detected	Week 1	Week 5	Week 9	Week 13	Week 17	Week 25	Follow-up (week 26 to 52)	Time to detection of secondary *KRAS* mutation (weeks)	Time from detection of secondary *KRAS* mutation to Disease Progression (weeks)
1	WT	NMD	**G12V**	NMD	NMD	NMD	NMD	**5**	43	**498**	17	16
			G12C	NMD	NMD	NMD	NMD	**5**	54	**431**		
			G12A	NMD	NMD	NMD	NMD	**2**	17	**317**		
			G12R	NMD	NMD	NMD	NMD	NMD	6	**36**		
2	WT	NMD	NMD	NMD	NMD	NMD	NMD	NMD		NMD		
3	G12D	NMD	NMD	NMD	NMD	NMD	NMD	NMD		NMD		
4	WT	NMD	**G12R**	NMD	NMD	NMD	NMD	NMD	NMD	**4**	34	Concurrent
5	WT	NMD	**G12D**	NMD	NMD	NMD	NMD	NMD		**13**	26	Concurrent
6	WT	NMD	NMD	NMD	NMD	NMD	NMD	NMD		NMD		
7	WT	NMD	NMD	NMD	NMD	NMD	NMD	NMD		NMD		
8	G13D	**G13D**	NMD	**23**	NMD	**100**	**119**			**385**		
9	WT	NMD	NMD	NMD	NMD	NMD	NMD	NMD	NMD	NMD		
10	WT	NMD	**G12V**	NMD	**23**	**46**	**3**	**46**	12	**37**	5	19
11	WT	NMD	NMD	NMD	NMD	NMD	NMD	NMD		NMD		
12	WT	NMD	**G12C**	NMD	NMD	NMD	NMD	NMD	25	**80**	25	Concurrent
			G12A	NMD	NMD	NMD	NMD	NMD	5	**20**		
13	WT	NMD	NMD	NMD	NMD	NMD	NMD	NMD	0	NMD		
14	WT	NMD	NMD	NMD	NMD			NMD	0	NMD		
15	WT	NMD	**G12V**	NMD	NMD	NMD	NMD	NMD		**127**	22	Concurrent
16	WT	NMD	NMD	NMD	NMD	NMD		NMD	NMD	NMD		
17	WT	NMD	NMD	NMD	NMD		NMD	NMD	NMD	NMD		
18	WT	NMD	NMD	NMD	NMD	NMD	NMD	NMD		NMD		
19	WT	NMD	NMD	NMD	NMD	NMD	NMD	NMD				
20	G13D	**G13D**	NMD	**411**	**146**		**1215**			**2484**		
21	WT	NMD	**G12V**	NMD	NMD	NMD	NMD			**16**	18	Concurrent
22	WT	NMD	**G12S**	NMD	NMD	NMD	NMD	**24**			17	Concurrent
			G12C	NMD	NMD	NMD	NMD	**3**				
			G12A	NMD	NMD	NMD	NMD	**8**				
			G12D	NMD	NMD	NMD	NMD	**4**				
23	WT	NMD	NMD	NMD		NMD	NMD	NMD		NMD		
24	WT	NMD	**G12A**	NMD	NMD	NMD	NMD	NMD		**3**	26	29
25	WT	NMD	NMD	NMD	NMD	NMD	NMD	NMD				
26	WT	NMD	NMD	NMD	NMD	NMD	NMD	NMD	NMD	NMD		
27	WT	NMD	NMD	NMD	NMD	NMD	NMD	NMD	NMD	NMD		
28	G12D	**G12D**	NMD	**810**	**518**	**806**				**984**		

* NMD = No Mutation Detected in the evaluated sample; blank values represent samples that were not available at the indicated time point

Supplementary Table 3. Tumor Burden and CEA data

CEA Levels:

#	w0	w8	w12	w16	w20	w24	w32	w40	Follow-up
1	4366.0	158.0	87.0	307.0		1014.0			3279.0
2	3526.0	149.0	50.0	42.0		122.0			92.0
3	194.2		268.0	364.7					462.6
4	4.9	0.6		1.8		2.3	4.4		6.4
5	4.8	2.7	2.7	3.5		2.7			3.6
6	154.0	164.0	65.0	61.0		56.0			55.0
7	25.0	2.9	2.1	6.3		29.0			42.5
8	11.0	6.7	10.1						36.8
9	43.6		1.0			1.0	1.9	4.8	10.5
10	40.7	7.2	5.8	8.6		16.6			9.1
11	16578.0	5069.0	2015.0	864.0		1217.0			2252.0
12	231.0	36.3	36.7	69.5	180.0	420.3			756.5
13	51.5	5.1	6.1	6.9		27.6			53.6
14	33.4			1.3		1.1			1.8
15	2454.0	805.0	504.0	569.0	1164.5	1628.0			1584.0
16	389.8		40.6	42.4		137.6			183.0
17	203.0	4.7	2.9	7.3		17.5	34.5		169.1
18	352.2	31.2	23.2	22.9	34.5				114.8
19	1.6	1.2		0.9					
20	190.5		346.5						521.5
21	27.1	4.5	5.4	515.0					9.8
22	73.5	51.6	50.6	35.9					
23	133.6	36.3	19.1	15.5		10.8	22.3		40.4
24	22.6	7.4	6.6	7.1		9.2			23.3
25	5.9	2.5	3.4	3.4					
26	281.1	73.3		48.7		43.5	60.6	116.7	164.9
27	13.9	3.6	3.3	3.0		3.7	4.8		5.8
28	25.8								19.1

Blank cells indicate timepoints for which no data were available

Total cross-sectional area (mm^2) of index lesions included in disease response assessment

#	w0	w8	w12	w16	w20	w24	w32	w40	Follow-up
1	13986	9094	7950	7050		7752			
2	24280	9774	9249	8585		10820			9907
3	6225	5904	7968	8316					9212
4	1240	204	342	360		550	594		
5	396	144	144	144		144			
6	13728	15865		9346		11194			
7	3290	1949	2114	2051		4190			
8	1849	1849	2401						
9	5923		3923			3572	3900		
10	1317	864	862	420		635			
11	5649	4411	3853	3506		3360			
12	7631	6375	4954	5236		7367			
13	12351	8274	8210	7612		7822			
14	3310	2039	1331	1265		2610	3386		
15	9657	4487	3865			3600			
16	6619	2964	2124	1911		3722			
17	2102	618	658	792		735	693		
18	12208	7757	7200	5556	4994				5209
19	748	154		121					
20	1714	2300	2959						
21	4484	4082	3847	3578					
22	38006	26596	27359	28512					
23	5580	4282	4444	4095		4025	3987		
24	3706	3594	3480	3285		2887			
25	2196	1749	1508	1687	1909				
26	6450	1864		1129		1730	2244	4620	
27	2799	2181	1892	1701		2088	2620		
28	1312	1698							

Blank cells indicate timepoints for which no data were available

Supplementary Table 4. Probability that the indicated mutation was absent prior to panitumumab therapy

Patient	*KRAS* mutation	Time (weeks)	*p*- value (*b* =0.25)	*p*- value (*b* =0.15)	*p*- value (*b* =0.35)
1	G12V	25	8E-1199	1E-1997	2E-856
1	G12C	25	2E-1505	2E-2508	2E-1075
1	G12A	25	2E-474	3E-790	5E-339
1	G12R	25	7.E-168	2.E-17	2E-1672
4	G12R	34	4.E-02	5.E-03	1.E-01
5	G12D	26	2.E-223	4E-372	7.E-160
10	G12V	25	4E-335	5E-558	1.E-239
12	G12C	25	3E-697	1E-1161	3E-498
12	G12A	25	5.E-140	6.E-233	3.E-100
15	G12V	22	1E-15203	6E-25399	6E-10860
21	G12V	18	6E-13378	5E-22296	7E-9556
22	G12S	17	6E-32621	9E-54368	7E-23301
22	G12C	17	3E-4078	1E-6796	3E-2913
22	G12A	17	4E-10874	4E-18123	2E-7767
22	G12D	17	2E-5437	7E-9062	4E-3884
24	G12A	26	4.E-52	2.E-86	2.E-37

Supplementary Table 5. Oligonucleotides primers and probes

Gene	Used for:	5'-Modification	Mutation	Sequence (5'-3')*
PCR Amplification Primers				
KRAS	**PCR forward primer**	**None**	**KRAS codons 12 & 13**	GATCATATTCGTCCACAAAATGATTC
KRAS	**PCR Reverse Primer**	**None**	**KRAS codons 12 & 13**	TGACTGAATATAAACTTGTGGTAGTTG
Ligation probes				
KRAS	**WT-specific probe**	**6-FAM**	**G12S**	TCC CGC GAA ATT AAT ACG AG CTA CGC CACC
KRAS	**Mutant-specific probe**	**HEX**	**G12S**	CTC TTG CCT AC GCC AGT
KRAS	**Common anchoring probe**	**Phosphate**	**G12S**	AGC TCC AAC TAC C GG TGT CCA CTA GTC ATG CTT
KRAS	**WT-specific probe**	**6-FAM**	**G12R**	TCC CGC GAA ATT AAT ACG AG CTA CGC CACC
KRAS	**Mutant-specific probe**	**HEX**	**G12R**	CT AC GCC AGG
KRAS	**Common anchoring probe**	**Phosphate**	**G12R**	AGC TCC AAC TAC C GG TGT CCA CTA GTC ATG CTT
KRAS	**WT-specific probe**	**6-FAM**	**G12C**	TCC CGC GAA ATT AAT ACG AG CTA CGC CACC
KRAS	**Mutant-specific probe**	**HEX**	**G12C**	CTA CGC CAC A
KRAS	**Common anchoring probe**	**Phosphate**	**G12C**	AGC TCC AAC TAC C GG TGT CCA CTA GTC ATG CTT
KRAS	**WT-specific probe**	**6-FAM**	**G12D**	ATG GAG AAC TTG ACG TCC T C CTA CGC CAC
KRAS	**Mutant-specific probe**	**HEX**	**G12D**	TGCCT +ACGC+C+AT
KRAS	**Common anchoring probe**	**Phosphate**	**G12D**	CAG CTC CAA CTAC GG TGT CCA CTA GTC ATG CTT
KRAS	**WT-specific probe**	**6-FAM**	**G12A**	ATG GAG AAC TTG ACG TCC T C CTA CGC CAC
KRAS	**Mutant-specific probe**	**HEX**	**G12A**	CCT ACGC C AG
KRAS	**Common anchoring probe**	**Phosphate**	**G12A**	CAG CTC CAA CTAC GG TGT CCA CTA GTC ATG CTT
KRAS	**WT-specific probe**	**6-FAM**	**G12V**	ATG GAG AAC TTG ACG TCC T C CTA CGC CAC
KRAS	**Mutant-specific probe**	**HEX**	**G12V**	CCT ACG CCA A
KRAS	**Common anchoring probe**	**Phosphate**	**G12V**	CAG CTC CAA CTAC GG TGT CCA CTA GTC ATG CTT
KRAS	**WT-specific probe**	**6-FAM**	**G13D**	ATG GAG AAC TTG ACG TCC T C CTT GCCTACGC
KRAS	**Mutant-specific probe**	**HEX**	**G13D**	CTT GCCTACGT
KRAS	**Common anchoring probe**	**Phosphate**	**G13D**	CACCAGCTCCAAC GG TGT CCA CTA GTC ATG CTT
BEAMing probes				
KRAS	**Detecting beads containing either WT or mutant sequences**	**ROX**	**G12S**	TGACGATACAGCTAATTCA
KRAS	**WT-specific probe**	**Cy3**	**G12S**	TGGAGCTGGTGGCGT
KRAS	**Mutant-specific probe**	**Cy5**	**G12S**	TGGAGCTAGTGGCGT
KRAS	**Detecting beads containing either WT or mutant sequences**	**ROX**	**G12R**	TGACGATACAGCTAATTCA
KRAS	**WT-specific probe**	**Cy3**	**G12R**	TGGAGCTGGTGGCGT
KRAS	**Mutant-specific probe**	**Cy5**	**G12R**	TGGAGCTCGTGGCGT
KRAS	**Detecting beads containing either WT or mutant sequences**	**ROX**	**G12C**	TGACGATACAGCTAATTCA
KRAS	**WT-specific probe**	**Cy3**	**G12C**	TGGAGCTGGTGGCGT
KRAS	**Mutant-specific probe**	**Cy5**	**G12C**	TGGAGCTTGTGGCGT
KRAS	**Detecting beads containing either WT or mutant sequences**	**ROX**	**G12D**	TGACGATACAGCTAATTCA
KRAS	**WT-specific probe**	**Cy3**	**G12D**	GGAGCTGGTGGCGTA
KRAS	**Mutant-specific probe**	**Cy5**	**G12D**	GGAGCTGATGGCGTA
KRAS	**Detecting beads containing either WT or mutant sequences**	**ROX**	**G12A**	TGACGATACAGCTAATTCA
KRAS	**WT-specific probe**	**Cy3**	**G12A**	GGAGCTGGTGGCGTA
KRAS	**Mutant-specific probe**	**Cy5**	**G12A**	GGAGCTGCTGGCGTA
KRAS	**Detecting beads containing either WT or mutant sequences**	**ROX**	**G12V**	TGACGATACAGCTAATTCA
KRAS	**WT-specific probe**	**Cy3**	**G12V**	GGAGCTGGTGGCGTA
KRAS	**Mutant-specific probe**	**Cy5**	**G12V**	GGAGCTGTTGGCGTA
KRAS	**Detecting beads containing either WT or mutant sequences**	**ROX**	**G13D**	TGACGATACAGCTAATTCA
KRAS	**WT-specific probe**	**Cy3**	**G13D**	AGCTGGTGGCGTAGGC
KRAS	**Mutant-specific probe**	**Cy5**	**G13D**	AGCTGGTGACGTAGGC

* indicates LNA linkages; red font indicates additional nucleotides appended to the ends of the common anchoring or WT-specific probes. Upon electrophoresis, the extra nt on the 5' end of the WT probes render the WT-specific ligation products larger than the mutant-specific ligation products.

Supplementary Table 6. Total circulating cell-free DNA levels (ng/ul)

Subject	Week 1	Week 5	Week 9	Week 13	Week 17	Week 25	Follow-up (week 26 to 52)
1	1.43	5.23	0.10	0.60	0.27	1.09	5.07
2	2.18	0.70	0.09	0.18	0.56		0.26
3	2.25	0.56	1.03	1.11			3.11
4	1.12	0.34	0.32	0.09	0.08	0.20	0.16
5	0.09	0.05	0.07	0.11	1.02		0.56
6	0.56	0.84	0.18	0.22	0.28		1.94
7	0.10	0.31	2.74	0.24	0.52		0.16
8	0.22	0.32	2.63	1.35			15.97
9	1.17	0.14	0.12	1.12	0.30	1.85	0.30
10	5.51	0.10	0.05	0.06	0.03	0.08	0.11
11	2.05	0.32	0.16	0.07	0.05		0.22
12	0.02	0.13	0.09	0.21	0.47	0.06	1.08
13	0.13	0.08	0.16	0.06	0.14	0.12	0.12
14	0.88	0.91			0.41	0.42	0.19
15	0.95	0.25	0.75	0.74	0.94		2.68
16	0.02	14.39	4.05		0.70	0.36	0.09
17	0.09	0.21		0.15	0.06	0.15	0.19
18	0.20	0.66	0.08	0.74	0.42		0.45
19	0.31	0.14	0.32	0.40	0.42		
20	0.39	0.07		1.04			0.06
21	0.39	0.39	0.07	0.05			0.41
22	0.52	0.38	0.26	0.16	0.14		
23	0.55		0.17	0.08	0.27		0.04
24	0.32	0.79	0.28	0.07	0.04		0.10
25	1.38	0.07	0.22	2.06	0.37		
26	0.16	1.41	0.92	1.53	0.58	0.34	0.39
27	0.52	0.12	0.07	0.07	1.70	0.17	0.62
28	1.11	0.25	1.73				0.64

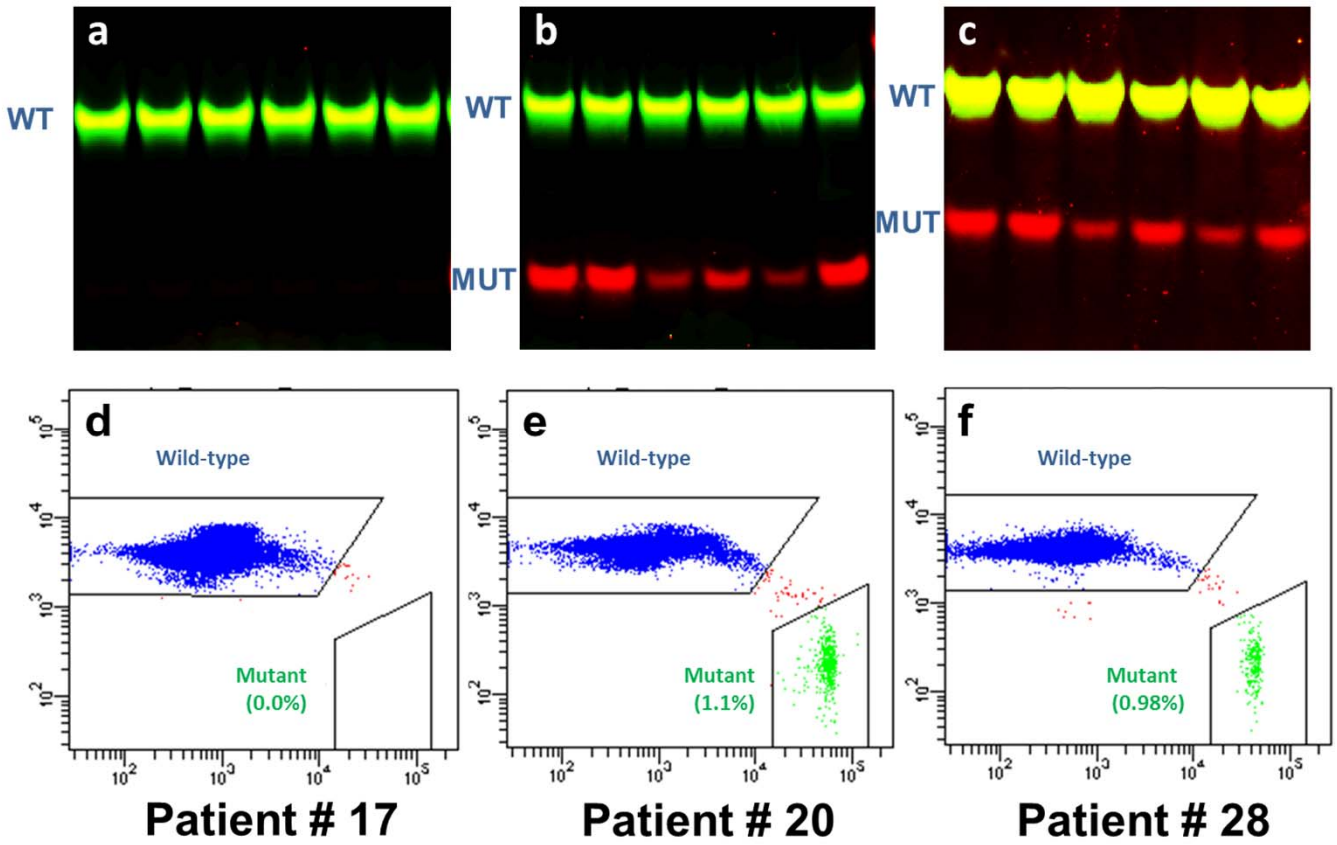

Supplementary Fig. 1. Ligation and BEAMing assays used to detect circulating *KRAS* mutations. **a, b, c**, Each lane represents the results of ligation of one of six independent *KRAS*-specific PCR products, each containing 100 template molecules from the indicated patients' pre-treatment serum samples. The wild-type ligation products contain 6-carboxyfluorescein-labeled oligonucleotide probes that ligate to an unlabeled oligonucleotide only when wild-type alleles are present. The mutant (MUT) ligation products contain hexachlorofluorescein-labeled oligonucleotide probes that ligate to the same unlabeled oligonucleotide only when mutant alleles are present. The fluorescent images of denaturing acrylamide gels in which the ligation products were size-separated are shown. **d, e, f,** *KRAS*-specific PCR products were used as templates for BEAMing in which each template was converted to a bead containing thousands of identical copies of the template[12]. After hybridization to Cy3- or Cy5-labeled oligonucleotide probes specific for wild-type or mutant sequences, respectively, the beads were analyzed by flow cytometry. Beads whose fluorescence spectra lie between the wild-type and mutant-containing beads result from inclusion of both wild-type and mutant templates in the aqueous nanocompartments of the emulsion PCR. See Materials and Methods for additional details. **a, d**: Patient #17; **b, e**: Patient #20; **c, f**: Patient #28. The mutant probes used in **a, b, d,** and **e** were specific for *KRAS* cDNA nt 38A and the mutant probes used in **c** and **f** was specific for *KRAS* cDNA nt 35A. The fraction of beads representing mutant templates are indicated for each patient.

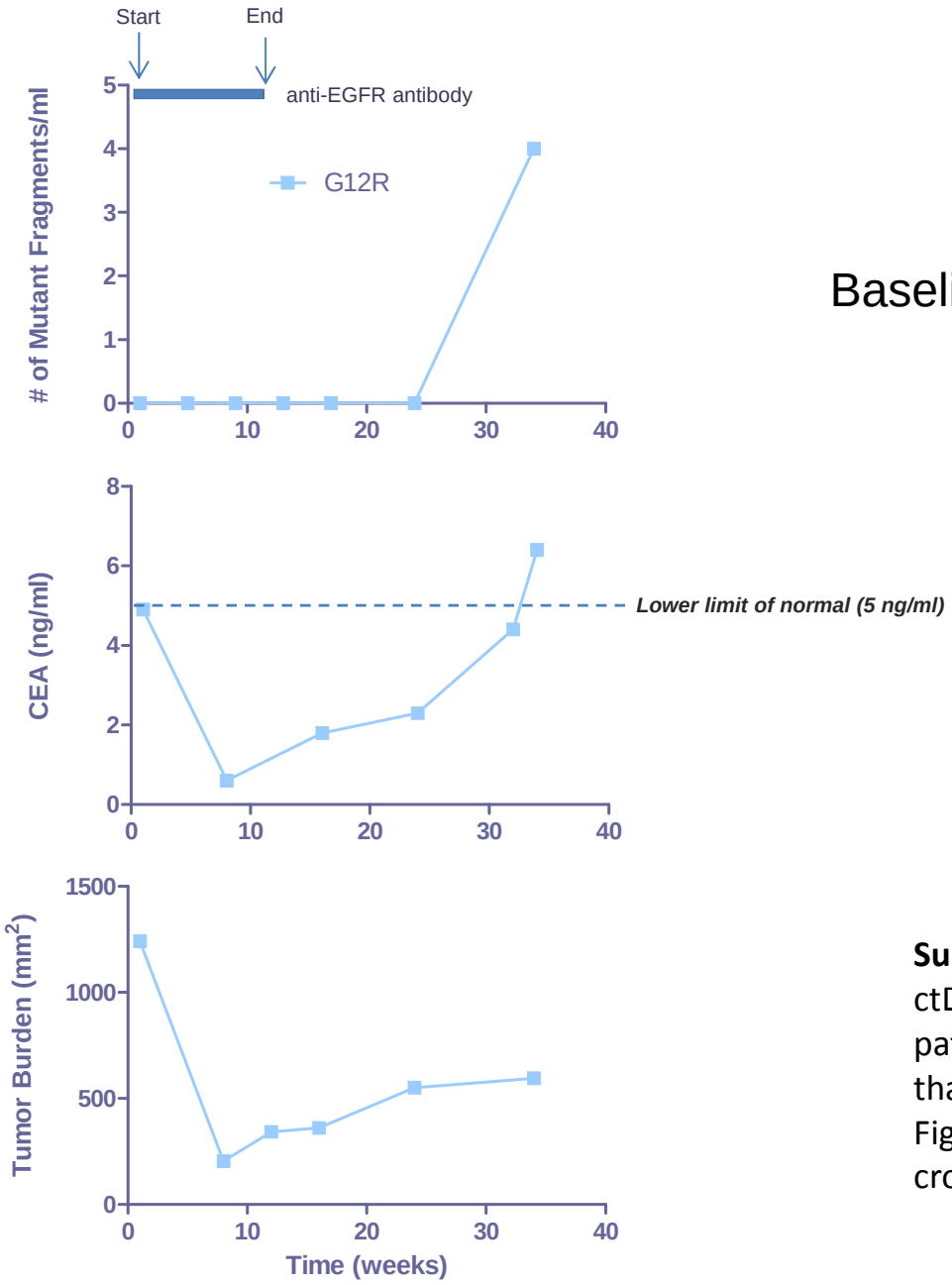

Patient # 4

Baseline KRAS Status: WT

Supplementary Fig. 2. Time course of ctDNA, CEA, and tumor burden for all the patients in which ctDNA was detected (other than Patients 1 and 12, which are depicted in Fig. 1). Tumor burden refers to the aggregate cross-sectional diameter of the index lesions.

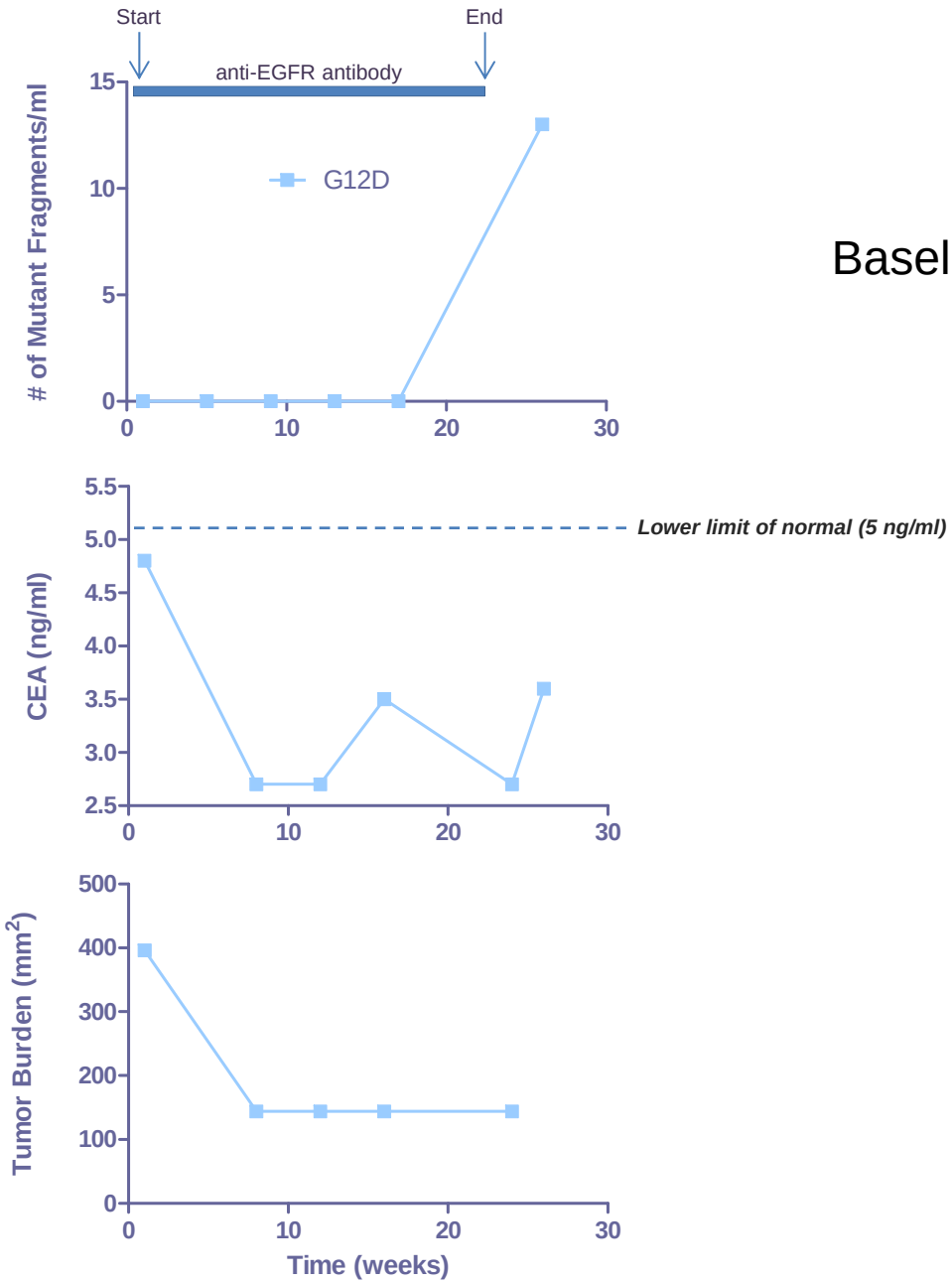

Patient # 5

Baseline KRAS Status: WT

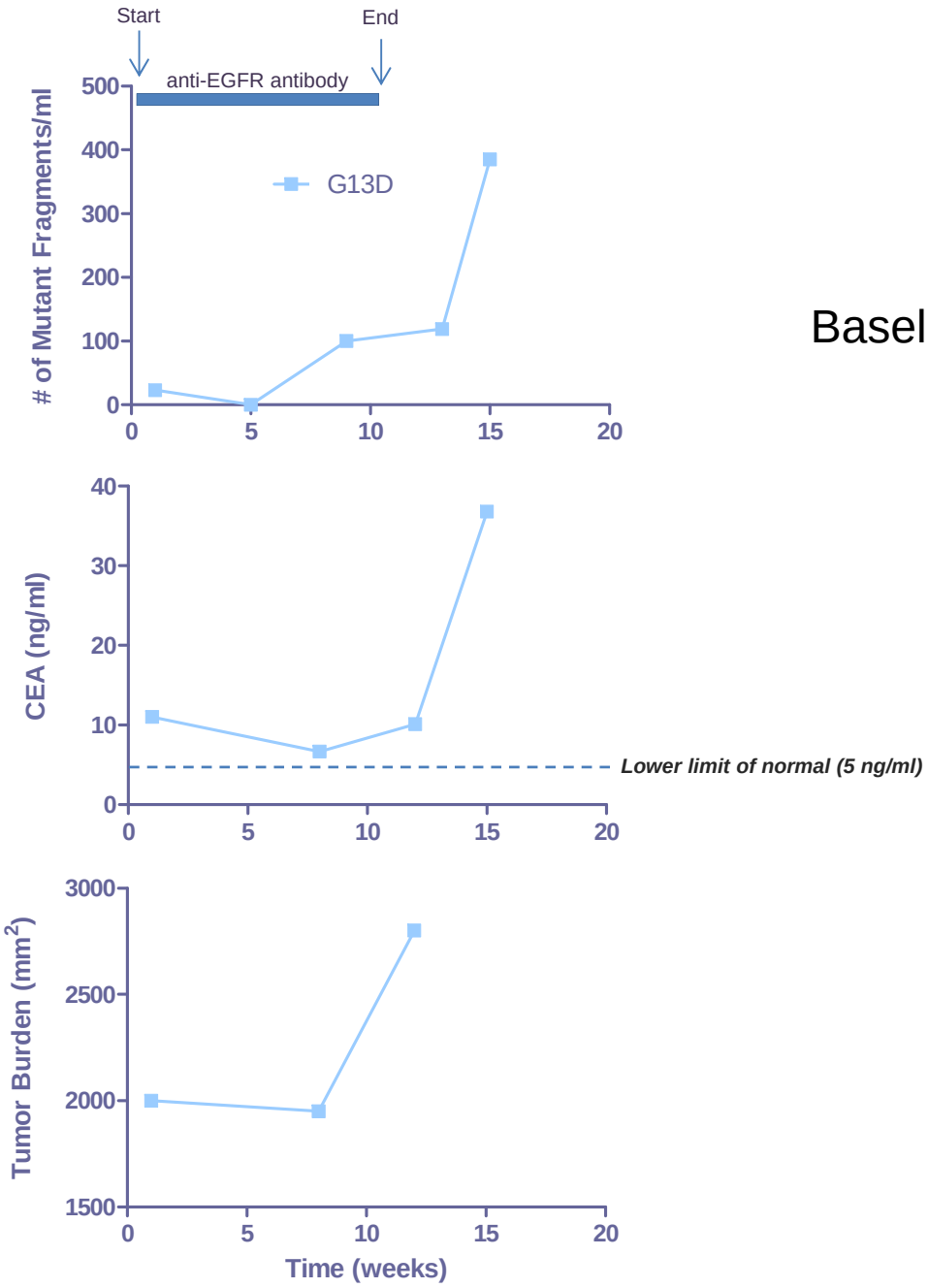

Patient # 8

Baseline KRAS Status: Mutant

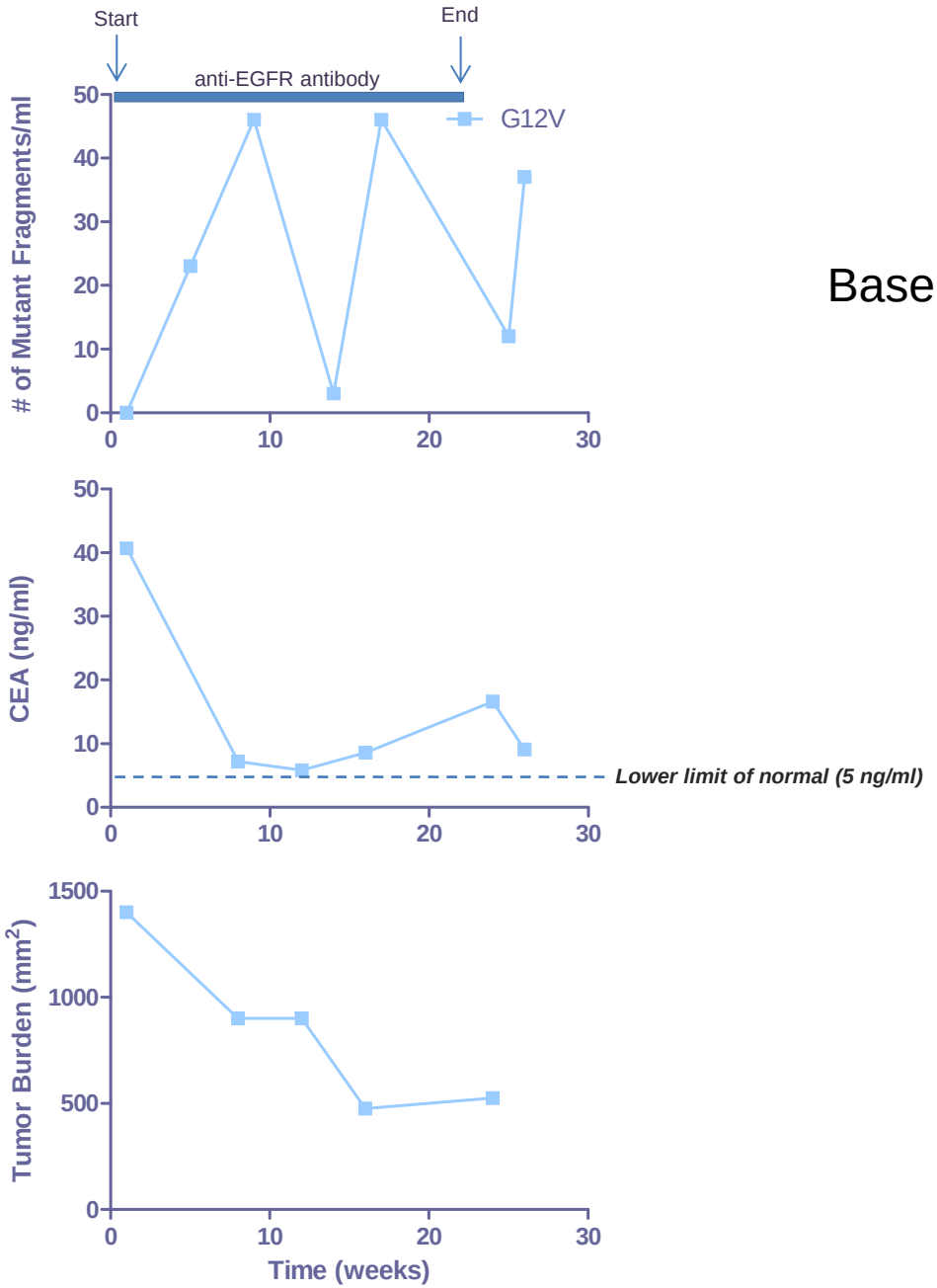

Patient # 10

Baseline KRAS Status: WT

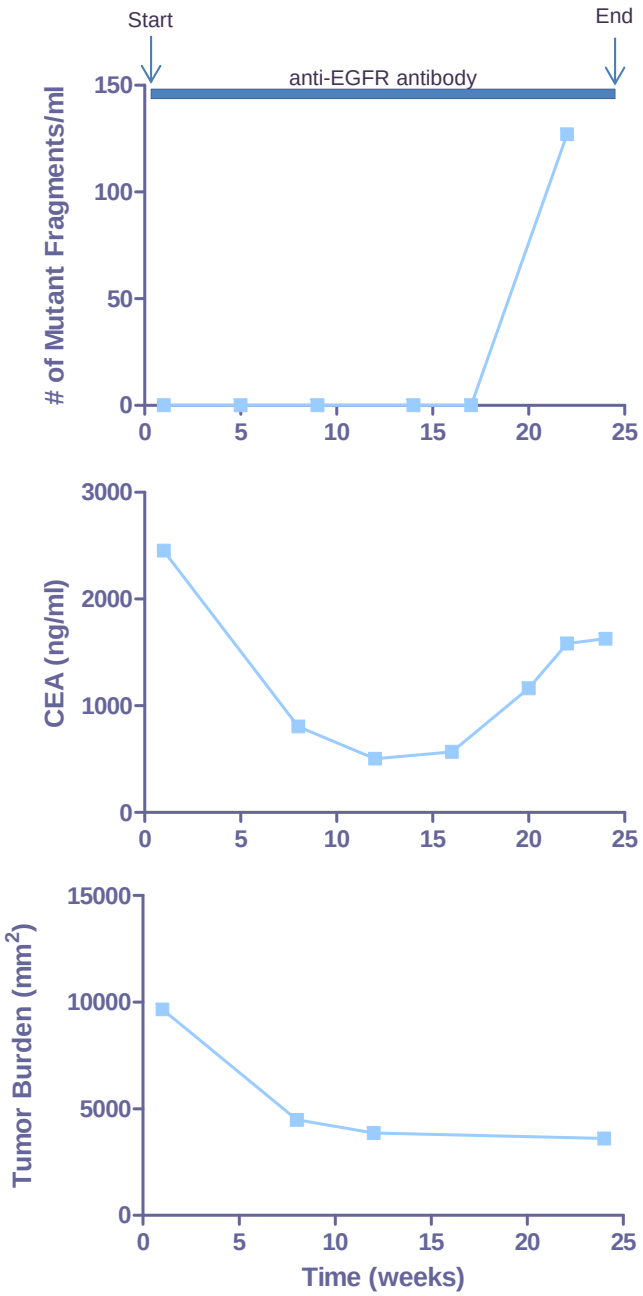

Patient # 15

Baseline KRAS Status: WT

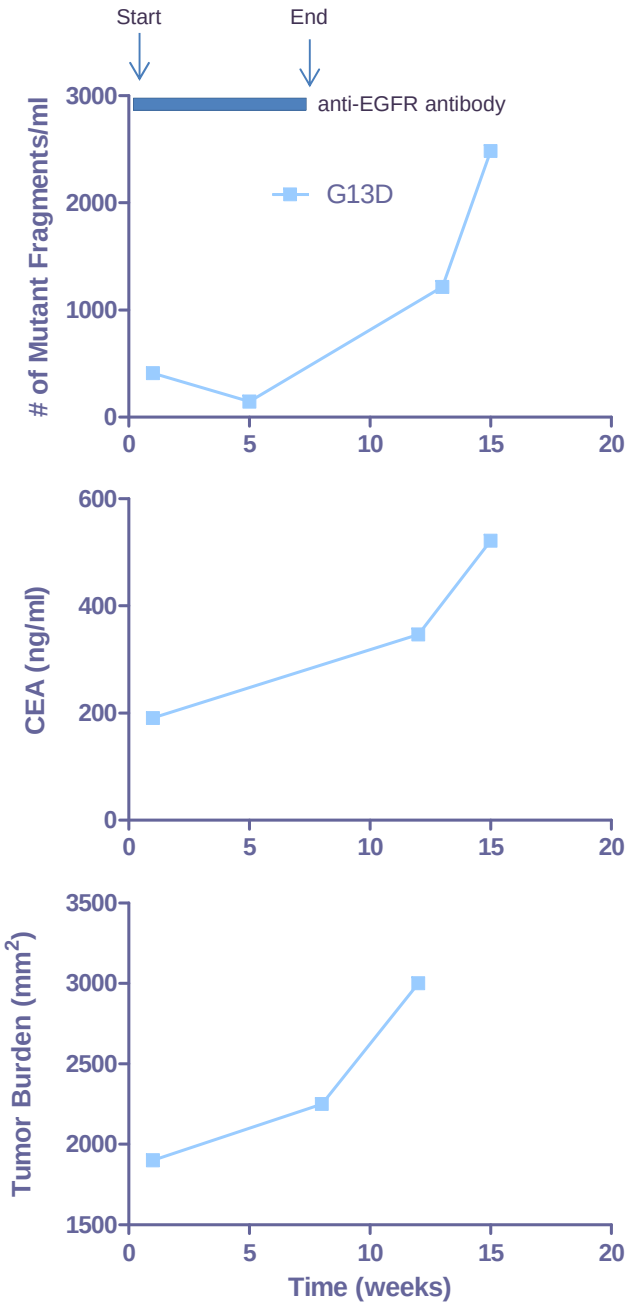

Patient # 20

Baseline KRAS Status: Mutant

DIAZ ET AL.

SUPPLEMENTARY FIGURE 2

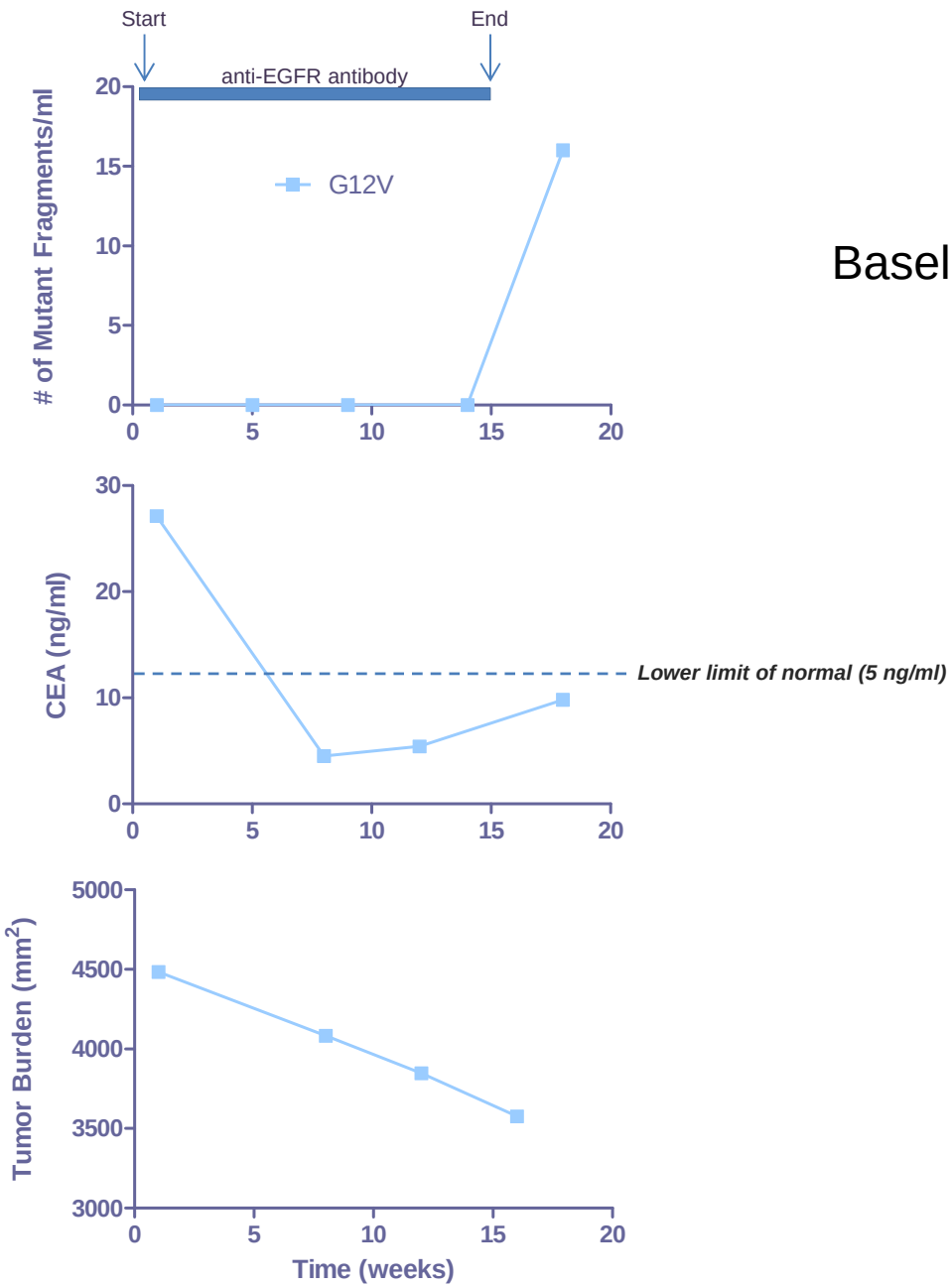

Patient # 21

Baseline KRAS Status: WT

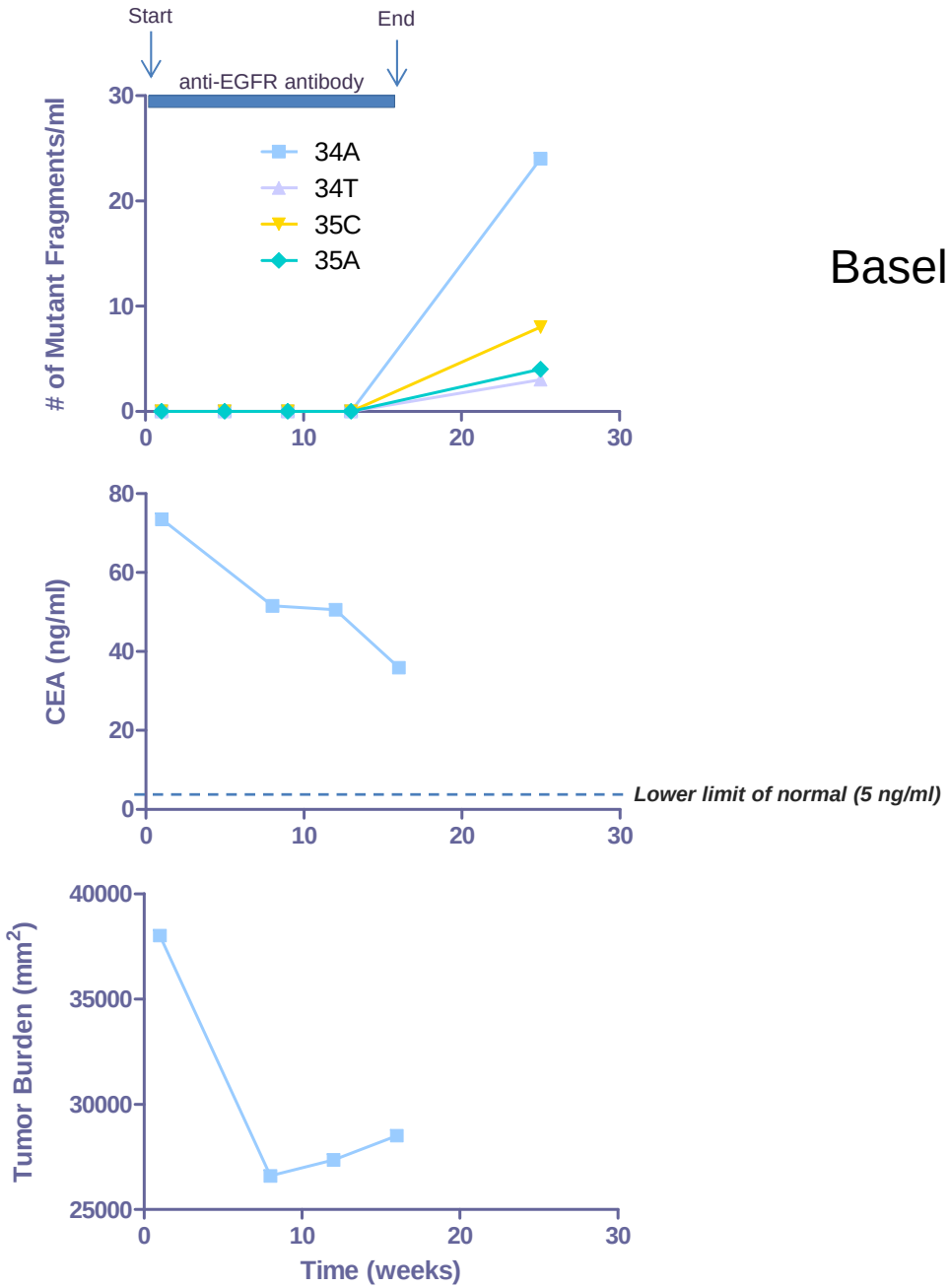

Patient # 22

Baseline KRAS Status: WT

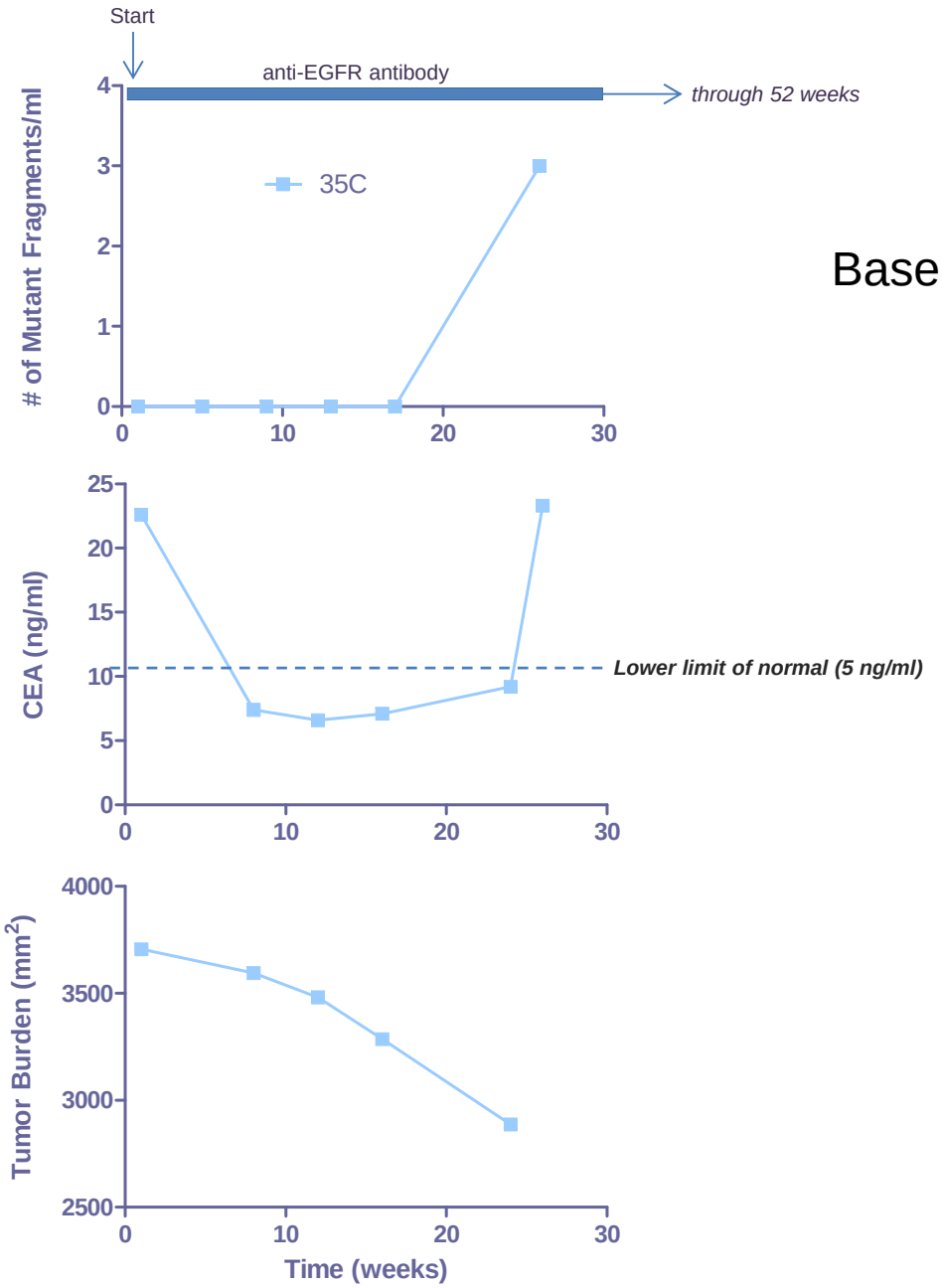

Patient # 24

Baseline KRAS Status: WT

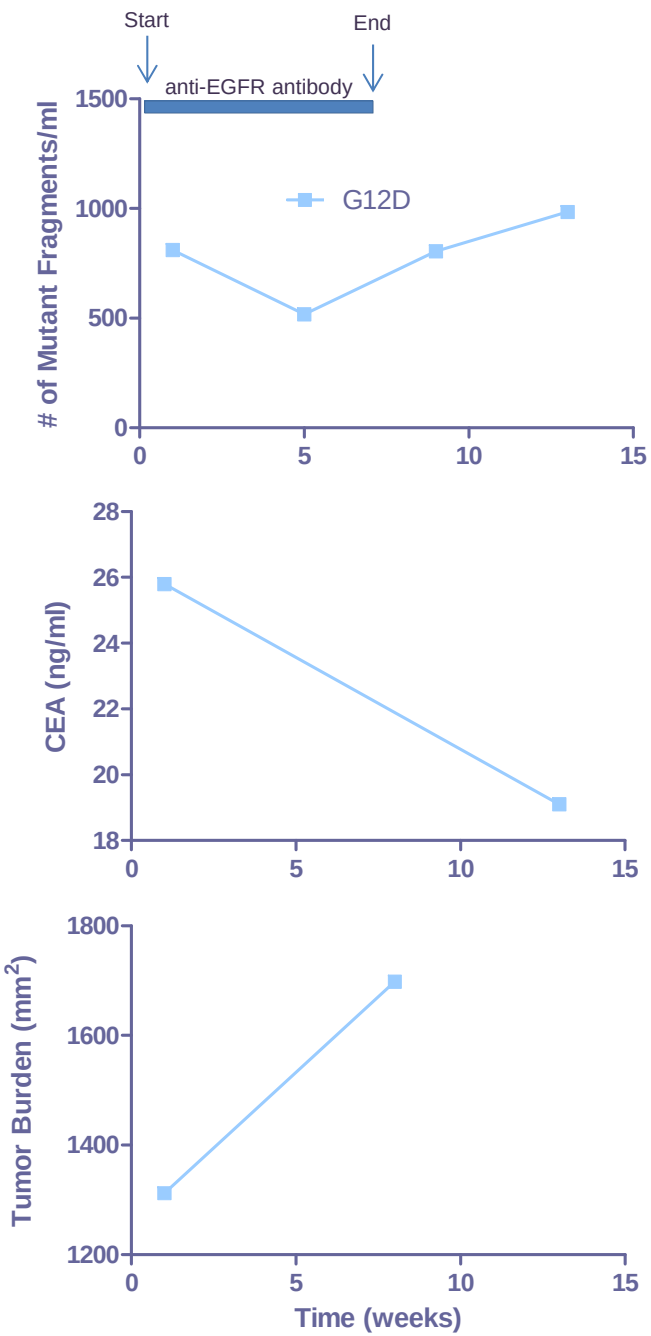

Patient # 28

Baseline KRAS Status: Mutant

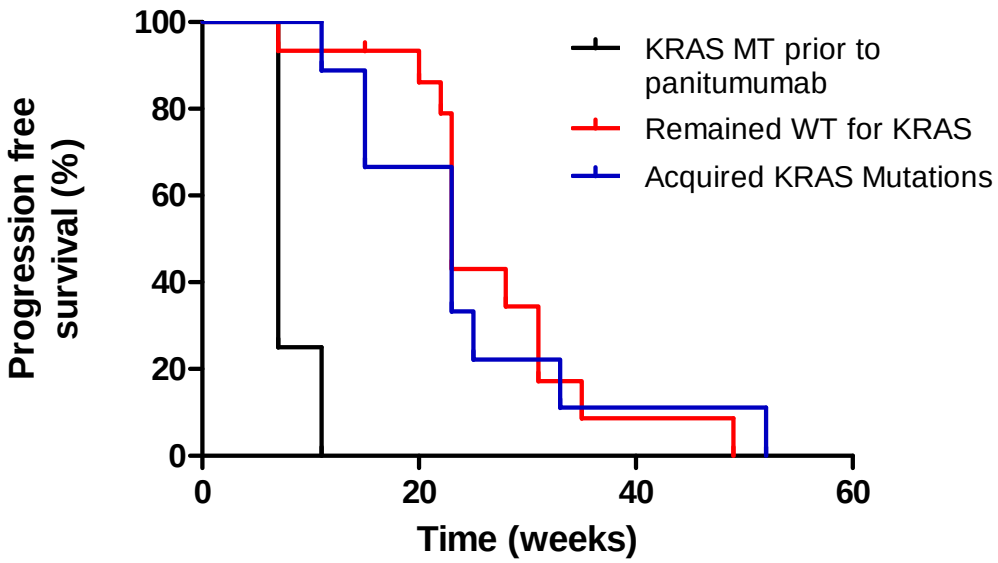

Supplementary Fig. 3. Kaplan-Meier Estimates of progression free survival in three groups of patients treated with panitumumab. (*Black*) patients whose tumors were *KRAS*-mutant prior to initiating therapy, (*Red*) patients whose tumors were wild-type for *KRAS* prior to starting therapy with panitumumab and *did not* develop detectable secondary mutation in *KRAS*, and (*Blue*) patients whose tumors patients whose tumors were wild-type for *KRAS* prior to starting therapy with panitumumab and *did* develop a detectable mutation in *KRAS*. The progression-free survival was not different among patients who did or did not develop *KRAS* mutations during treatment (Hazard ratio 0.9; 95% CI 0.3366 to 2.453; p=0.85; Log-Rank Test).

Supplementary Appendix

1 Statistical test to confirm presence of KRAS-mutated cells at start of treatment

We are interested in the question of whether there were pre-existing KRAS-mutated cells at the time that treatment was started. We take the case that KRAS-mutated cells were absent at the start of treatment as our null hypothesis H_0; the alternative hypothesis H_1 is that they were present.

We use a branching process model, described below, to test the null hypothesis. We perform this test separately for each KRAS mutation in each patient. Using our model, we compute an upper bound on the probability $\Pr[\Theta|H_0]$, where Θ is the event that a number of KRAS-mutated cells greater or equal to the observed number are present in the tumor at the time of observation. We use $\Pr[\Theta|H_0]$ as a p-value for this test. We reject H_0 if $\Pr[\Theta|H_0] < 0.05$.

1.1 Branching process model

We model the dynamics of KRAS-mutated cells by a branching process (Coldman and Goldie, 1983, 1986; Iwasa et al., 2006) with birth rate b and death rate d. We let $\tilde{X}_t$ denote the number of KRAS-mutated cells conditioned on nonextinction of this population. A result of Durrett and Moseley (2010) implies that, as $t \to \infty$, the quantity $e^{-(b-d)t}\tilde{X}_t$ converges to a random variable V, where V is exponentially distributed with mean $b/(b-d)$.

Using this result, we can write

$$\Pr[\tilde{X}_t \geq N] \approx \Pr[V \geq e^{-(b-d)t}N] = \exp\left(-\frac{b-d}{b}e^{-(b-d)t}N\right),$$

where the approximation is accurate for large t. We conclude that

$$\Pr[\Theta|H_0] \leq \exp\left(-\frac{b-d}{b}e^{-(b-d)T}N\right),$$

where T is the time at which the number of KRAS-mutated cells, N, is measured.

1.2 Estimation of parameter values

We use the observed data to estimate the growth rate, $b-d$, of KRAS-mutated cells. This growth rate is equal to the change in the log number of cells per unit time. We therefore estimate this growth rate as

$$b - d \approx \frac{\text{total change in log number of cells}}{\text{total change in time}}.$$

To compute this average, we used the data from Patients 1 and 12, for which there were multiple KRAS mutations that were observed to grow over the course of two or more measurements. This yielded an estimate of $b-d \approx 0.069$ as average growth rate of KRAS-mutated cells per day. We also computed the growth rates separately for each lesion in Patients 1 and 12.

We initially assume $b = 0.25$, which corresponds to one cell division every four days, and obtain d from the estimated value of $b-d$. We also repeat our analysis for $b = 0.15$ and $b = 0.35$ to test the sensitivity of our results to this parameter.

As described in the main text, we estimate that each KRAS-mutated fragment detected per milliliter of blood corresponds to 4.4×10^7 KRAS-mutated cells.

2 Probability that resistant cells exist at start of treatment under generalized Luria-Delbrück distribution

To complement the above hypothesis tests, we also calculate the probability that resistant cells exist at the start of treatment, under a Luria-Delbrück distribution generalized to incorporate cell death (Dewanji et al., 2005). This distribution assumes a particular model of tumor development, in which the

population of sensitive cells grows exponentially, and resistance mutations arise stochastically. A slower pattern of growth (but still leading to the same tumor size at the start of treatment) would be expected to yield more resistance mutations (Luebeck and Moolgavkar, 1991). In contrast, the hypothesis tests described above make no assumptions on the dynamics of the sensitive cell population.

From this point forward we use the following notation and parameter values (unless otherwise specified):

- $M = 10^9$ is number of tumor cells at the start of treatment,
- $b = 0.25$ is the division rate of both sensitive and resistant cells,
- $d = 0.181$ is the death rate, so that the growth rate is $b - d = 0.069$ (as inferred above from the observed dynamics of circulating KRAS-mutated fragments),
- $u = 42 \times 10^{-9}$ is the total rate at which resistance mutations are generated (assuming 42 possible mutations conferring resistance, as estimated in the main text, and a mutation rate of 10^{-9} per cell division).

Using the generalized Luria-Delbrück distribution proposed by Dewanji et al. (2005; or equivalently, the formulas of Iwasa et al., 2006), we calculate the likelihood that no resistant cells exist prior to treatment to be 4×10^{-33}. Thus, under this model, resistance is almost certainly present at the start of treatment.

3 Distribution of waiting times until resistance can be detected

This generalized Luria-Delbrück distribution can also be used to obtain the distribution of waiting times until resistance mutations become detectable in circulating DNA. To obtain this distribution, we first used the methods of Dewanji et al. (2005) to numerically calculate the size distribution of the resistant cell population at the start of treatment. We then assume that the resistant cell population grows exponentially (deterministically) once treatment starts. This deterministic assumption is justified since, for the above parameter values, the number of resistant cells at the start of treatment is

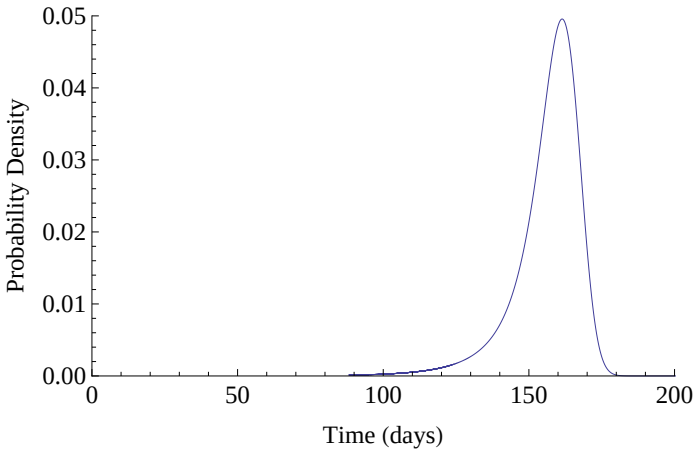

Figure 1: Predicted probability distribution of times from when treatment starts until resistance mutations become observable in circulating DNA. Predictions are based on the Lea-Coulson model with death introduced by Dewanji et al. (2005), or equivalently, the branching process model of Iwasa et al. (2006). Tumor growth rates were inferred from the growth in observed KRAS fragments over time in different lesions; otherwise, parameters were not fit to the data.

likely to be large. (For instance, there is a 99% chance that there are at least 276 resistant cells when treatment starts.) We used 4.4×10^7 for the number of resistant cells for which resistance mutations become observable in circulating DNA.

The resulting distribution has a mean of 156 days (22 weeks), with a standard deviation of 11 days. The 95% confidence interval spans from 126 days (18 weeks) to 172 days (25 weeks). The probability density function for this distribution is plotted in Figure 1.

Our analytic results were confirmed through simulation of the birth-death branching process with mutation (Coldman and Goldie, 1986; Iwasa et al., 2006), using the above parameter values. In these simulations, the exact branching process is followed for clonal populations smaller than 10^4, and deterministic exponential growth approximations are used for larger populations. These simulations yielded a mean of 157 days and a standard deviation of 12 days for the waiting time until resistance become detectable.

These results are a close match to the observed data, in which resistance mutations were first observed at Week 17 in some cases and Week 25 in others. In particular, the sharpness of this distribution helps explain the striking similarity, across patients and lesions, in the times at which resistance mutations become detectable.

To incorporate the possibility that not all cells in a lesion are actively dividing, we repeated this analysis using $M = 10^8$ as the number of actively dividing tumor cells at the start of treatment (one-tenth of the total number of cells in a detectable lesion). This yielded an expected time of 200 days (29 weeks), with a standard deviation of 17 days. The assumption that all (or almost all) tumor cells are actively dividing—that is, $M = 10^9$ as above—better fits the observed data.

4 Size of the largest clonal subpopulation of resistant mutants

Next we obtain an analytical estimate for the size of the largest clonal subpopulation of resistant cells. We assume that the largest clonal subpopulation is the progeny of the first resistance mutation to arise and survive stochastic drift. This is reasonable, since resistance mutations beyond the first are likely to arise significantly later, after this first subpopulation has grown

substantially.

We use the result of Iwasa et al. (2006) that the collection of tumor sizes at which resistance mutations are produced can be viewed as a homogenous Poisson process on $[1, M]$ with intensity $u/(1 - d/b)$. Each such mutation survives stochastic drift with probability $1 - d/b$, so the tumor sizes at which mutations that survive stochastic drift arise are produced can be viewed as a Poisson process on on $[1, M]$ with intensity u. Since M is large and u is small, we can replace the interval $[1, M]$ by $[0, M]$, without losing much accuracy.

Let M_1 denote the size of the tumor when the first mutation that survives stochastic drift is produced. Then M_1 is exponentially distributed with mean u^{-1} (since M_1 corresponds to the first event in a Poisson process with intensity u). By the time that the total tumor cell population reaches size M, the size of the clonal subpopulation initialed by this mutation can be approximated by MV/M_1, where V is an exponentially distributed random with mean $b/(b - d)$. (This follows from the results of Durrett and Moseley, 2010.)

Let Y_1 denote the size of the clonal subpopulation initiated by the first mutation that survives stochastic drift, conditioned on $M_1 \leq M$ (i.e., this mutation arises before the tumor reaches size M). Using the above results, we obtain the cumulative distribution function $F(y)$ of Y_1 by

$$\begin{aligned}
1 - F(y) &= \Pr[Y_1 \geq y] \\
&\approx \Pr\left[\frac{MV}{M_1} \geq y \middle| M_1 \leq M\right] \\
&= \int_{z=0}^{M} \text{Prob. Density}\left[M_1 = z | M_1 \leq M\right] \times \Pr\left[V \geq \frac{yz}{M}\right]\, dz \\
&= \int_{z=0}^{M} \frac{ue^{-zu}}{1 - e^{-Mu}} \exp\left(-\frac{yz}{M}\frac{b-d}{b}\right)\, dz \\
&= \frac{u}{1 - e^{-Mu}} \int_{z=0}^{M} \exp\left(-z\left(u + \frac{y}{M}\frac{b-d}{b}\right)\right)\, dz \\
&= \frac{Mu}{1 - e^{-Mu}} \left(Mu + y\frac{b-d}{b}\right)^{-1} \left(1 - \exp\left(-Mu - y\frac{b-d}{b}\right)\right).
\end{aligned}$$

The expected size of this clonal subpopulation can be calculated as

$$E[Y_1] \approx \int_0^M yF'(y)\, dy \approx 2237,$$

for the given parameter set. Simulations of the birth-death branching process (as described in Section 3 above) confirmed the size of the largest clone to be ~ 2300.

We can compare this to the total expected number of resistant mutants, $E[Y]$, which can be calculated using Eqn. (13) of Dewanji et al. (2005) or Eqn. (10) of Iwasa et al. (2006):

$$E[Y] \approx 3241.$$

Thus most (69%) of the resistant population is comprised of a single clonal type.

We can also vary the number of possible mutations conferring resistance by varying u; for example, in the case of four mutations conferring resistance we would use $u = 4 \times 10^{-9}$. The results are shown in the following table:

Number of mutations conferring resistance	$E[Y_1]$	$E[Y]$	$E[Y_1]/E[Y]$
4	252	309	81%
10	584	772	76%
42	2237	3241	69%
100	4575	7717	65%

References

Coldman, A. J., and J. H. Goldie. 1983. A model for the resistance of tumor cells to cancer chemotherapeutic agents. Mathematical Biosciences 65:291–307.

———. 1986. A stochastic model for the origin and treatment of tumors containing drug-resistant cells. Bulletin of Mathematical Biology 48:279–292.

Dewanji, A., E. Luebeck, and S. Moolgavkar. 2005. A generalized luria–delbrück model. Mathematical Biosciences 197:140–152.

Durrett, R., and S. Moseley. 2010. Evolution of resistance and progression to disease during clonal expansion of cancer. Theoretical Population Biology 77:42 – 48.

Iwasa, Y., M. A. Nowak, and F. Michor. 2006. Evolution of resistance during clonal expansion. Genetics 172:2557–2566.

Luebeck, E. G., and S. H. Moolgavkar. 1991. Stochastic analysis of intermediate lesions in carcinogenesis experiments. Risk Analysis 11:149–157.